Effects of inlet conditions and surface roughness on the performance of transitions between square and rectangular ducts of the same cross-sectional area

E. I. Dekam and J. R. Calvert*

A study has been made of the effects of inlet conditions and surface roughness on the performance of transitions between square and rectangular ducts of the same cross-sectional area. The conditions at entry were varied by using different approach lengths of straight duct and by means of a square screen of woven wire cloth. The surface roughening was accomplished by coating the surface of the transition with graded waterproof silicon carbide paper, whose surface roughness was measured with a Talysurf 4 instrument. All tests were run at Reynolds number 10^5.

The results indicate that the static pressure loss coefficient significantly increases as the inlet boundary layer thickness increases. This variation is a function of aspect ratio at the rectangular end; the loss coefficient rises as the aspect ratio falls. The pressure drop slightly increases when the wall surface is roughened and is higher at low aspect ratios.

Keywords: *ducts, transitions, inlet conditions, surface roughness*

Introduction

The flow head losses associated with shape changes in constant area ducts are usually significant. Flow in transition ducts is of considerable practical importance since transitional systems are used in a wide range of applications. For example, transitional systems are used when it is necessary to join rectangular (or square) to rectangular ducts of the same cross-sectional area. These transitions may be made up of flat panels and will have a maximum cross-sectional area at their longitudinal midpoint, which may be significantly larger than the end areas.[1] Thus they are classified as divergent-convergent transitions, where both accelerations and decelerations are involved.[2] Alternatively, it is possible to design transitions with curved walls, which have constant cross-sectional area.[3]

We have previously published experimental results for the pressure loss in divergent-convergent transitions between square and rectangular ducts, and vice versa.[2] There it was found that the static pressure loss coefficient consistently falls as Reynolds number rises and is higher for the longer sections ($L/D=2$) than for the shorter ($L/D=1$). There also is a significant increase in the pressure loss coefficient as the aspect ratio falls, and it is significantly higher for rectangular to square transitions than for square to rectangular.

The pressure loss in constant area (curved wall) transitions is generally less than that in the divergent-convergent cases.[4]

The previous experiments were concerned with transitions with very smooth surfaces and thin inlet boundary layers, conditions unlikely to be realistic in many applications. To investigate their effects, the experiments reported here have been carried out with rougher surfaces (CLA roughness height about 0.01 mm) and artificially thickened inlet boundary layers. These should enable the previous results to be applied to a wider range of applications.

* Department of Mechanical Engineering, University of Southampton, Southampton, S09 5NH, England

Received 20 February 1986 and accepted for publication 22 October 1986

0142-727X/87/040287-06$03.00

Previous work

Surface roughness

Persh and Bailey[5] investigated the effect of surface roughness on the performance of a 23° conical diffuser with a 2:1 ratio of exit to inlet area and a constant-area tailpipe 3.5 inlet diameters, and with an inlet boundary-layer thickness of approximately 5% of the inlet diameter. Their results show the static pressure recovery at the diffuser exit diminished slightly as the extent of roughness was extended upstream from the exit to the condition in which 97% of the diffuser length was roughened.

Velocity profile

Comprehensive data have been reported in the effect of inlet flow conditions on diffuser performance. Various classes of inlet velocity profiles have been considered (see Figure 1). Waitman, Reneau, and Kline[6] studied the effect of inlet conditions on performance of plane-walled diffusers. Specifically, they looked at the effect of thickening the inlet boundary layer (Figure 1a), increasing the inlet turbulence intensity, and creating a single momentum deficient region located both symmetrically (Figure 1c) and unsymmetrically (Figure 1f). They concluded that the static pressure recovery is a function of inlet boundary layer conditions. Reductions in recovery occur as the inlet boundary layer is thickened. Wolf and Johnston[7] also studied the effect of nonuniform inlet velocity profiles—uniform and severly nonuniform shear flows—(Figures 1a–1c, 1e, and 1f) on flow regimes and performance in plane-walled diffusers. They used damping screens for velocity-profile control. They reported that diffusers with nonuniform inlet velocity profiles having a low velocity core-flow region near one or both walls, such as uniform shear flows (Figures 1a, b) and nonuniform shear flows of the jet (Figure 1e) and step-shear (Figure 1f) type, exhibit similar decreased performance when compared to diffusers having uniform inlet velocity profiles. Tyler and Williamson[8] performed a series of experiments with conical and annular diffuser geometries using inlet velocity profile distortion created

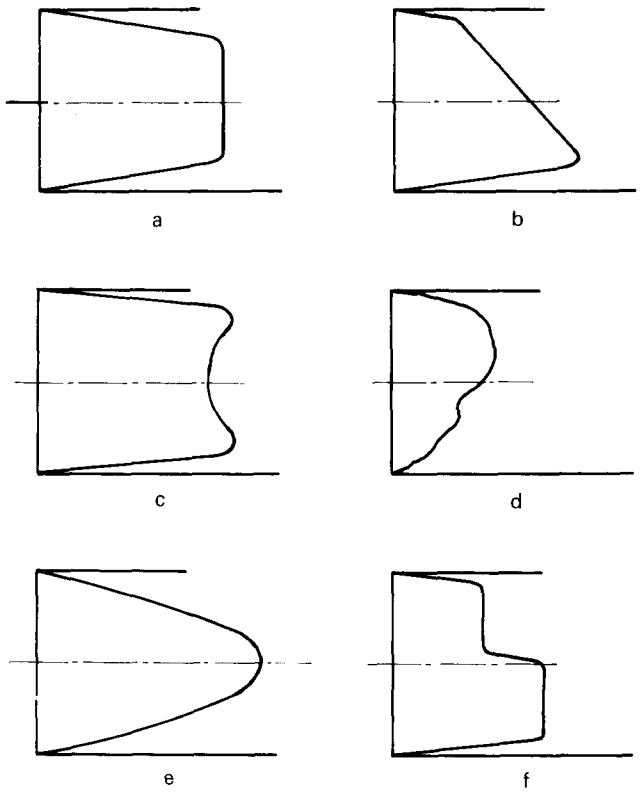

Figure 1 Typical inlet velocity profiles: (a) symmetrical, uniform inlet velocity over a core region outside the wall boundary layer region; (b) unsymmetrical, uniform shear flows (flows with constant vorticity in the core); (c) centrally located wake-type (nonuniform shear flows); (d) severely nonuniform velocity profile (nonuniform shear flows); (e) symmetrical, nonuniform profile (jet flow); (f) step-shear velocity profile

by cross flow at the inlet section. A marked effect of inflow distortion on optimum diffuser geometry was indicated.

Robertson and Ross[9] investigated the flow conditions in conical diffusers when preceded by 2-diameter, 5-diameter, and 9-diameter lengths of straight pipe and well-faired, large area-ratio contraction. They reported that the extent of the boundary layer at the entrance to the diffuser is as important a factor in determining the diffuser flow as is the diffuser angle. Winternitz and Ramsay[10] studied the effect of inlet conditions on the performance of conical diffusers with 4:1 area ratio. The conditions at the entry were varied by using different approach lengths and by projecting annular screens of woven wire cloth. Their conclusion is that diffuser energy efficiency and other measures of diffuser effectiveness depend on the momentum thickness ratio at inlet, regardless of the inlet velocity profile. Johnston and Powars[11] presented some experimental results on effects caused by change of inlet blockage and aspect ratio on performance of straight-walled, two-dimensional diffusers with incompressible, steady flow. The inlet boundary layer displacement thickness was held constant for all of their tests, and the value of inlet blockage factor was controlled by varying the aspect ratio (by varying only the inlet duct width). The main observation is that the pressure recovery coefficient increased with increasing aspect ratio as expected, since inlet blockage decreased as aspect ratio increased.

Al-Mudafar, Ilyas, and Bhinder[12] have reported results of an experimental study on the influence of severely distorted velocity profiles (see Figure 1d) on the performance of straight two-dimensional diffusers. They obtained the desired velocity profile by using two rectangular section ducts with independently controllable valves upstream of the diffuser inlet duct, which was divided into two equal parts by a thin plastic strip. This strip can be moved to alter the mixing length upstream of the diffuser throat. They reported that the pressure recovery progressively deteriorates as the inlet velocity is distorted. Kaiser and McDonald[13] have studied the effect of centrally located "wake-type" inlet velocity profiles (see Figure 1c) on the inception of stall in two-dimensional plane-wall diffusers. They observed that diffusers with distorted inlet velocity profiles exhibit stall behavior quite different from that found in diffusers with uniform inlet profiles. Performance of conical diffusers with fully developed pipe flow at the entry has been discussed by Bradshaw[14] and Cockrell and Markland.[15] The reduction in diffuser pressure-recovery that occurs with increased thickness of the turbulent inlet boundary layer is studied by Sovran and Klomp.[16] They concluded that the blockage concept provides a method for comparing inlet velocity profiles in diffusers of different cross-sectional shape. This suggests the possibility of evaluating inlet effects for only one geometric type of diffuser and then applying the results to other cross-sectional forms.

Theory

Figure 2(a) shows the geometry of a square to rectangular transition. This may be treated as a diffusion from area A_1 to area A_2, followed by a contraction to area A_3 $(=A_1)$.[2] In the diffusing half, the pressure will rise because of diffusion and fall because of losses. The net effect may be either a rise or a fall. In the contracting half, the pressure will fall because of both contraction and losses. The overall pressure loss coefficient C may be expressed as

$$C=\frac{P_1-P_3}{1/2\rho u_{av}^2} \tag{1}$$

$$=\left[\left(\frac{E_1}{E_3}\right)^2-1\right]\left(\frac{1}{E_1}\right)^2+\frac{P_{om1}-P_{om3}}{1/2\rho u_{av}^2} \tag{2}$$

where $E=u_{av}/U$ and is the effective area fraction from which we may obtain the blocked area fraction $B=1-E$. E, B, and the

Notation

A	Cross-sectional area
a, b	Sides of rectangular section
B	Blocked area fraction
C	Static pressure loss coefficient
CLA	Centerline average
D	Inlet hydraulic diameter (square side)
E	Effective area fraction
g	Aspect ratio, $\frac{a}{b}$
L	Transition length
L_u	Inlet duct length (upstream)
P	Static pressure
P_{om}	Total pressure on streamline of maximum velocity
Re	Reynolds number
U	Maximum velocity
u	Local velocity
u_{av}	Average velocity
δ^*	Boundary layer displacement thickness
θ	Boundary layer momentum thickness
H	Boundary layer shape factor
ρ	Fluid density

Subscripts

1	At transition entry
2	At transition center
3	At transition exit

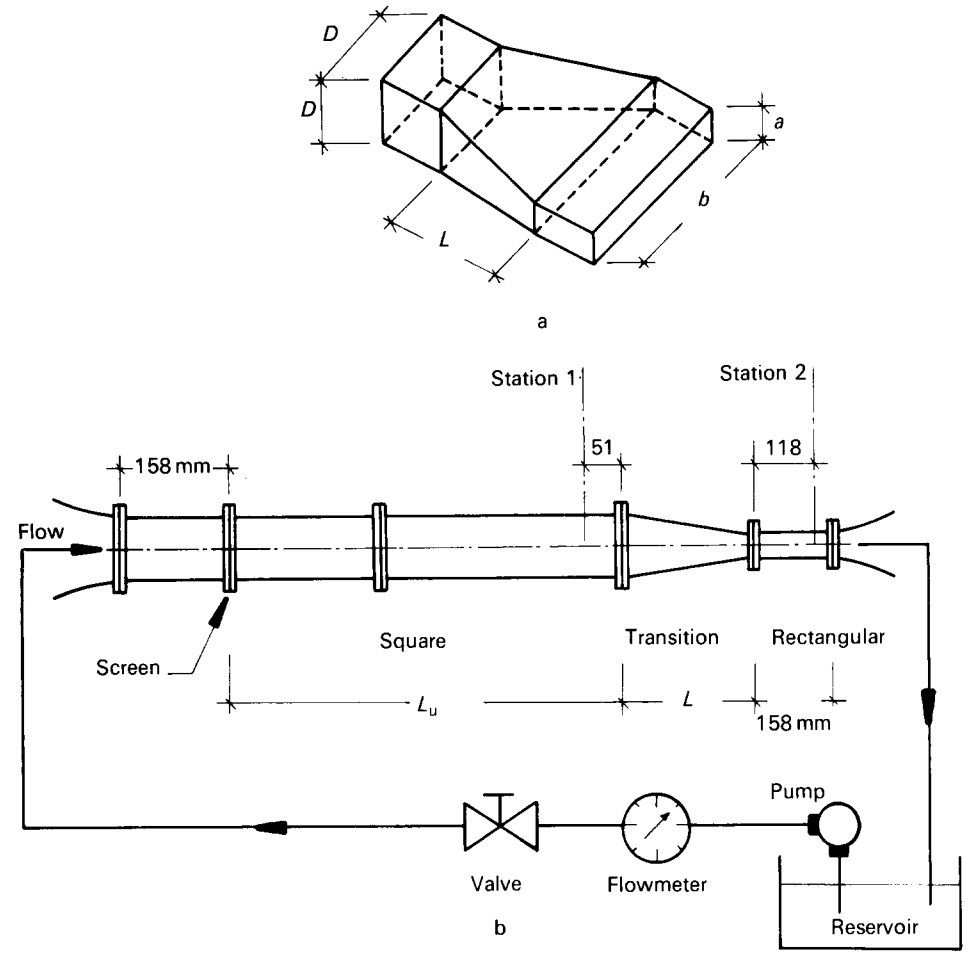

Figure 2 Test sections and rig: (a) transition between square and rectangular; (b) general arrangement of transition rig

boundary layer displacement and momentum thicknesses may be obtained from velocity traverses.

Apparatus and experiments

Tests were carried out in the water channel pump circuit that we previously described.[2] A general assembly diagram of the test sections is shown in Figure 2(b). The experimental test sections were square to rectangular transitions made of perspex. Waterproof silicon carbide paper was used to add internal wall roughness, measured by Talysurf 4. Both ends had 250 cm^2 cross-sectional area. Three different aspect ratios were used at the rectangular ends 0.3, 0.4, and 0.625. One length was used—158 mm ($L/D=1$). All tests were run at Reynolds number of approximately 10^5 based on the inlet hydraulic diameter, D.

The test sections were mounted between parallel ducts, which in turn, were attached to curved plywood entry-exit sections. Upstream of the test sections, a square screen of woven wire cloth (12 mesh, 25 s.w.g., mounted between the flanges of the contraction and the straight section), and different approach lengths of square duct were used to vary the boundary layer thickness and to produce variations in the inlet velocity distributions. Mean velocities were obtained from a turbine flowmeter in the water channel pump circuit.

Total pressures were measured with pitot probes mounted on a traverse gear well downstream of the test section, and static pressures were measured at wall tappings. Traverses were made in the approach and outlet ducts at stations 1 and 2, as indicated in Figure 2. Pressure differences were measured by an inclined differential water manometer with a resolution of 0.125 mm.

Results

Systematic data collected during the test program included observations of the flow patterns and measurements of static pressure distributions and velocity profiles. The flow patterns were determined by observing wool tufts (about 50 mm long) moved gradually over all the surfaces of the smooth transitions (the rough transitions were not transparent). The estimated maximum errors in the various measured quantities (except the measurements of low velocities, which were subject to larger errors) are all $\pm 1\%$ or less. The cumulative maximum errors in the derived quantities are estimated to be $\pm 5\%$ or less.

Varying the length of the inlet section and using wire mesh provided symmetric inlet boundary layers of varying thickness. The static pressure was approximately constant across the cross section in all cases.

Flow separation from the walls of a diffuser is the major cause of poor pressure recovery. However, none of the smooth transitions tested exhibited separation, although one of them (with $g=0.3$ and $B_1=0.31$) was close to this condition (see Figure 4).

Velocity profiles

Inlet velocity profiles were measured for each inlet duct length at station 1, and exit velocity profiles were measured at station 2 (see Figure 2b) in vertical and horizontal planes through the duct centerline.

Inlet velocity profile

In the square duct, no significant differences could be discerned between the inlet traverses in a vertical or horizontal plane.

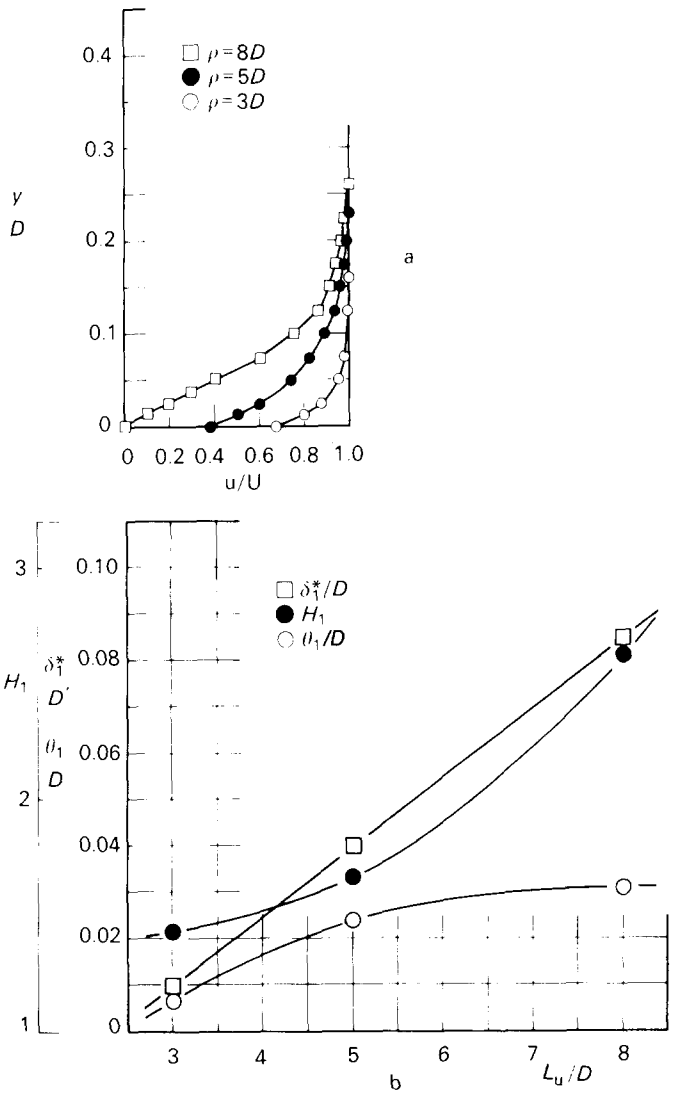

Figure 3 Inlet flow conditions: (a) inlet velocity profiles; (b) boundary layer parameters

Only the horizontal traverses are therefore presented. From these, the inlet boundary layer parameters δ_1^* and θ_1 were calculated. Figure 3(a) shows inlet velocity profiles for three different profile generators.

For each of the experimental velocity distributions, the displacement and momentum thicknesses were obtained by graphical integration. Figure 3(b) shows the growth of the inlet displacement and momentum thicknesses against the approach length. The inlet displacement thicknesses were approximately 13.4, 6.3, and 1.6 mm at, respectively, $L_u = 8D$, $5D$, and $3D$.

Figure 3(b) also shows the ratio H_1 of the inlet displacement thickness δ_1^* to the inlet momentum thickness θ_1— approximately, $H_1 = 2.6$ and 1.4 at $\delta_1^*/D = 0.085$ and 0.010, respectively.

Outlet velocity profiles

It is logical to compare outlet velocity traverses in different aspect ratio transitions of the same relative inlet lengths. Figure 4(a) presents horizontal outlet traverses for smooth transitions of different outlet aspect ratio for the same entrance conditions with $L_u = 8D$. The transition with aspect ratio 0.3 has the thickest boundary layer, whereas the transition with aspect ratio 0.625 has the thinnest boundary layer. For horizontal traverses, approximately, $\delta_3^* = 17.5$, 16.3, and 15.0 mm, and $H_3 = 3.1$, 2.8, and 2.2 at, respectively, $g = 0.3$, 0.4, and 0.625.

The transition outlet velocity profiles are influenced by the thickness of the entering boundary layer. Figures 4(b) and 4(c) show horizontal and vertical traverses at station 2 for a smooth transition with aspect ratio 0.4, for pipe-entrance lengths of 3, 5, and 8 diameters. These curves show a marked increase in effect with an increase in entrance boundary layer thickness. For horizontal traverses, approximately, $\delta_3^* = 16.3$, 8.1, and 3.1 mm, respectively, at $L_u = 8D$, $5D$, and $3D$. For vertical traverses, $\delta_3^* = 14.0$, 6.5, and 2.2 mm, respectively.

Effective and blocked area fractions

Figure 5(a) shows the change in effective area fraction between inlet and outlet, as a function of aspect ratio. The ratio E_1/E_3 falls as aspect ratio rises (the duct becomes more square) and increases with higher inlet boundary layer thickness. E_1/E_3 ranges from 1.14 down to 1.07 ($\delta_1^*/D = 0.085$ and 0.010, respectively) for rough transitions with $g = 0.3$. These ratios fall to approximately 1.13 and 1.04, respectively, in smooth transitions.

The curves shown in Figure 5(b) indicate that the blocked area fraction at the exit of the transitions is almost independent of roughness for given aspect ratio and entry condition. The variation increases as the inlet blocked area decreases, which implies that as the inlet blocked area (or δ_1^*/D) falls, the surface roughness effect rises and makes the outlet blocked area larger. It can be seen that the value of B_3 for rough transition with $g = 0.3$ is the highest value measured for all entry conditions.

Static pressure loss coefficient

Figure 6 shows the measured static pressure loss coefficient, C, for different inlet boundary layer thicknesses. This figure indicates that C increases as the inlet blocked area increases in all the transitions tested. For the same entry conditions, the effect of the surface roughness rises as aspect ratio falls. This may be because of the increase of the wall surface areas (the area increase is 6.3% and 12.9%, respectively, at $g = 0.4$ and 0.3) with the larger pair of the walls converging. This effect of surface roughness decreases as B_1 rises and matches the effects of surface roughness in pipe flow (see, for example, Miller).[17]

From the same data, the ratios of additional losses due to surface roughness to total losses in hydraulically smooth transitions may be obtained (Figure 7). For transitions with $g = 0.4$, these ratios are approximately 95.5%, 18.7%, and 3.9% at $B_1 = 0.05$, 0.15, and 0.31, respectively. This confirms that as B_1 falls, the effect of surface roughness becomes greater for all the transitions examined.

It is found that the frictional loss term $(P_{om1} - P_{om3})/(1/2\rho u_{av}^2)$ is approximately zero in the smooth and rough transitions tested because of the presence of potential flow core along their centerlines. Here, the influence of the surface roughness is accounted for by the velocity profile distortion loss term, which is a function of B.

Conclusions

Experimental results for the pressure loss in transitions between square and rectangular ducts of the same cross-sectional area are presented. Effects of inlet boundary layer thickness and surface roughness on the flow behavior in the transitions have been reported. The results indicate that the static pressure drop significantly increases as the inlet boundary layer thickness rises. For the same entry conditions, the pressure drop increases as the aspect ratio at the rectangular end falls. The frictional losses due to the presence of surface roughness rise as the inlet boundary layer thickness decreases, and at low inlet boundary layer thickness, the friction losses dominate.

It would also be of interest to study effects of unsymmetrical inlet velocity profiles such as step-shear and severely distorted profiles. This is practically important since blockage elements, such as heat exchangers and branching ducts, may produce this type of profile.

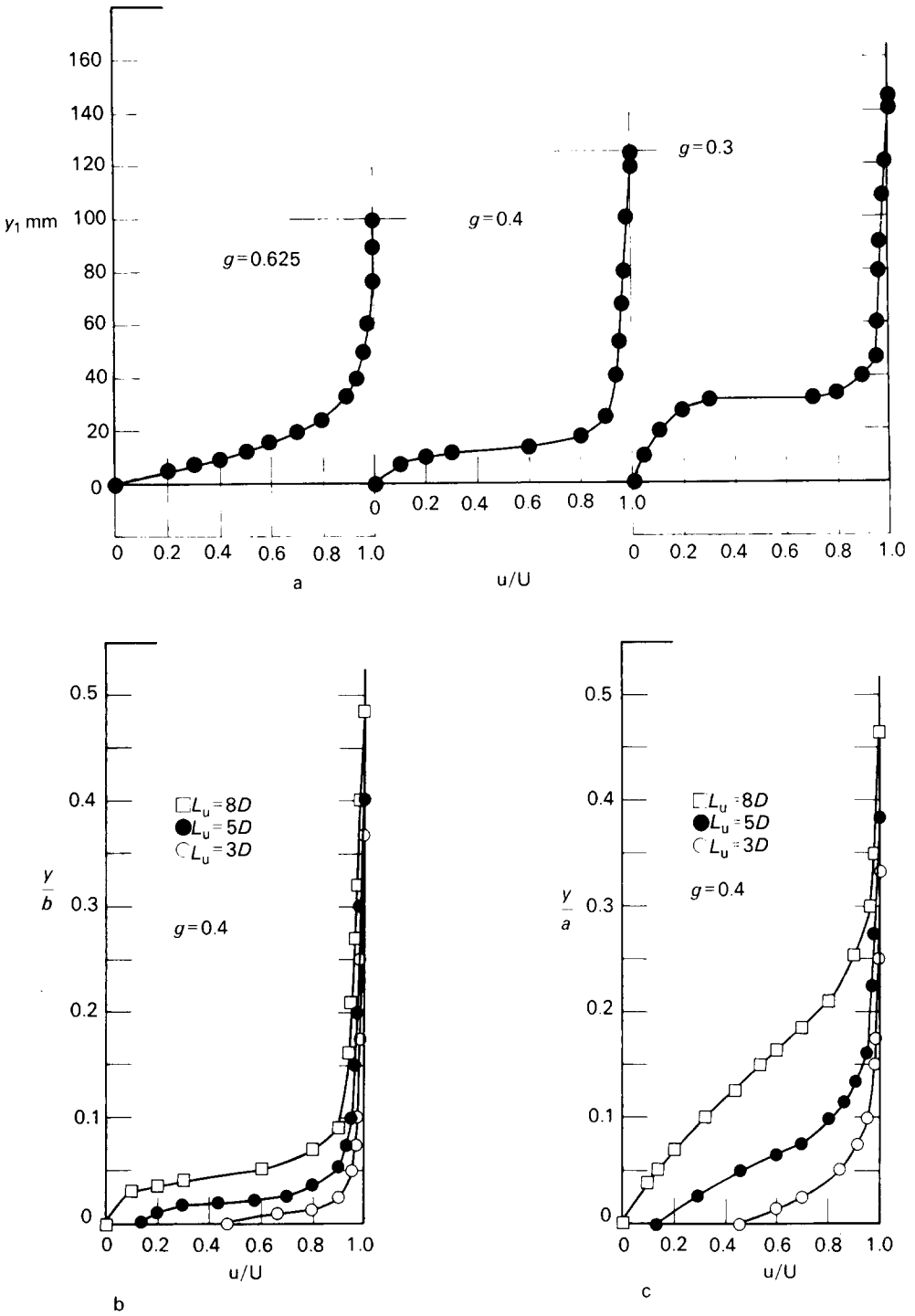

Figure 4 Outlet velocity profiles: (a) horizontal traverses with $L_u=8D$; (b) horizontal traverses with $g=0.4$; (c) vertical traverses with $g=0.4$

Acknowledgement

The authors are grateful to Mr. M. A. Batey, workshop supervisor, and his staff for the construction of apparatus.

References

1 Atilgan, M., and Calvert, J. R. Geometry of transition sections between ducts of equal area. *J. Wind Eng. and Ind. Aerod.*, 1980, 25–37.

2 Dekam, E. I., and Calvert, J. R. Pressure losses in transitions between square and rectangular ducts of the same cross-sectional area. *Int. J. Heat and Fluid Flow*, 1985, **6**(3), 212–216.

3 Dekam, E. I., and Calvert, J. R. Design of transition sections between ducts of equal area. *J. Wind Eng. and Ind. Aerod.*, in press.

4 Dekam, E. I., and Calvert, J. R. Effects of wall curvature on the performance of transition ducts. Submitted to *J. Wind Eng. and Ind. Aerod.*, 1986.

5 Persh, J., and Bailey, B. M. Effects of surface roughness over the downstream reigon of a 23 degrees conical diffuser. NACA TN 3066, Jan. 1954.

6 Waitman, B. A., Reneau, L. R., and Kline, S. J. Effects of inlet conditions on performance of two-dimensional subsonic diffusers. *J. Basic Eng.*, 1961, **83**, 349–360.

7 Wolf, S., and Johnston, J. P. Effects of nonuniform inlet velocity profiles on flow regimes and performance in two-dimensional diffusers. *J. Basic Eng.*, 1969, **91**(3), 462–475.

8 Tyler, R. C., and Williamson, R. G. Diffuser performance with distorted inflow. *Pro. Inst. Mech. Engrs.*, 1967–1968, **182**(3D), 1–11.

9 Robertson, J. M., and Ross, D. Effect of entrance conditions on diffuser flow. *Pro. ASMCE*, 1952, **78**, separate no. 141.

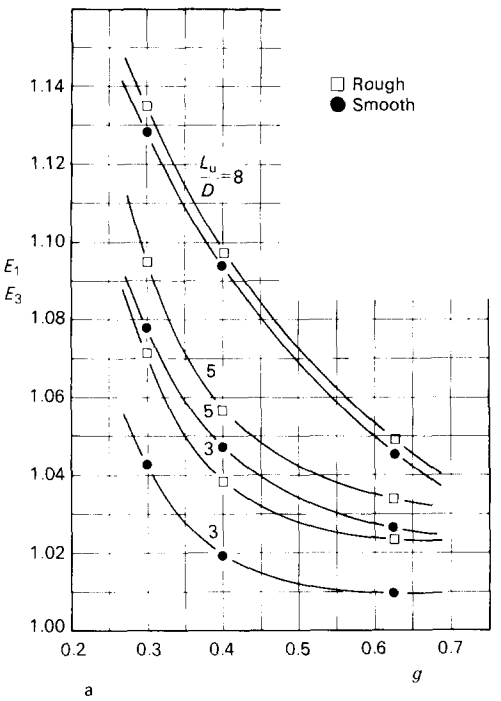

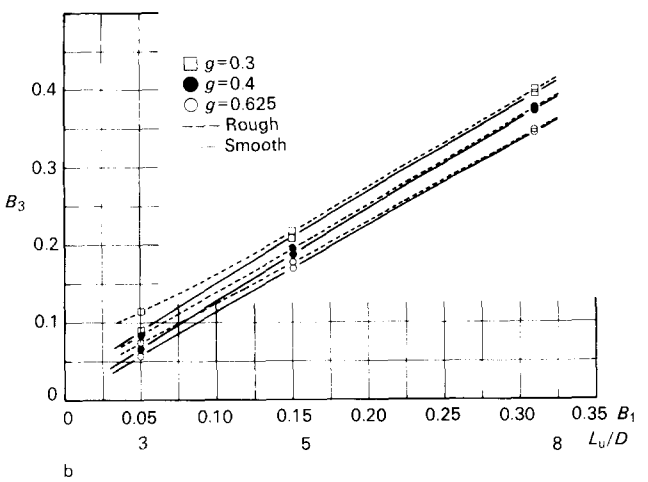

Figure 5 Effective and blocked area fractions: (a) outlet blocked area fraction; (b) effect of aspect ratio on effective area fraction

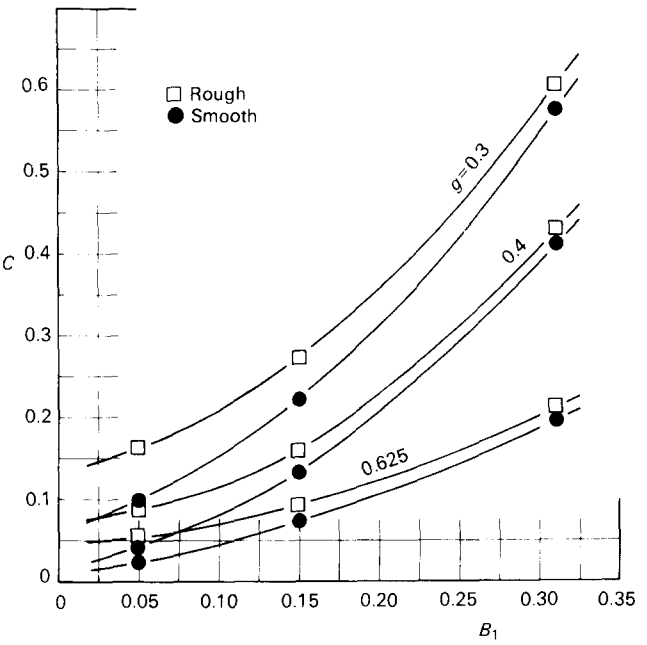

Figure 6 Effect of inlet blocked area on pressure loss coefficient

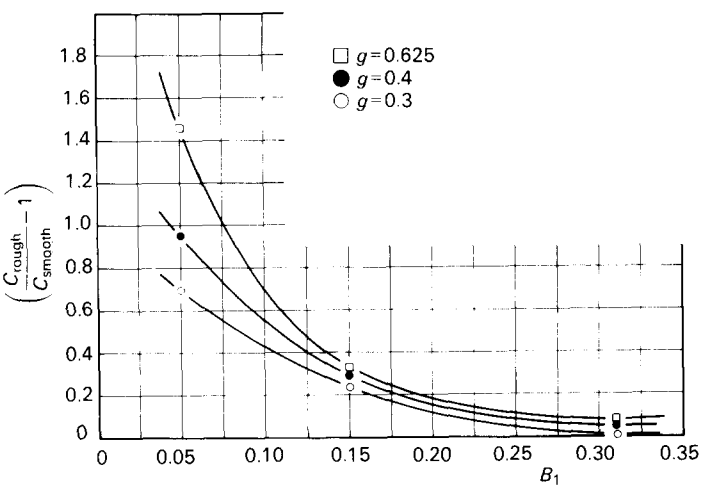

Figure 7 Ratio of frictional losses due to the presence of surface roughness to total losses in hydraulically smooth transitions

10 Winternitz, F. A. L., and Ramsay, W. J. Effects of inlet boundary layer on pressure recovery, energy conversion and losses in conical diffusers. *J. Royal Aero. Soc.*, 1957, **61**, 116–124.

11 Johnston, J. P., and Powars, C. A. Some effects of inlet blockage and aspect ratio on diffuser performance. *J. Basic Eng.*, 1969, **91**(3), 551–553.

12 Al-Mudafar, M. M., Liyas, M., and Bhinder, F. S. Investigation of flows in rectangular diffusers with flow distortion. *Trans. ASME*, 1982, 1–5.

13 Kaiser, K. F., and McDonald, A. T. Effects of wake-type nonuniform inlet velocity profiles on first appreciable stall in plane-walled diffusers. *J. Basic Eng.*, 1980, **102**, 283–289.

14 Bradshaw, P. Performance of a diffuser with fully-developed pipe flow at entry. *J. Royal Aero. Soc.*, 1963, **67**, 733.

15 Cockrell, D. J., and Markland, E. The effects of inlet conditions on incompressible fluid flow through conical diffusers. *J. Royal Aero. Soc.*, 1962, **66**, 51–53.

16 Sovran, G., and Klomp, E. D. Experimentally determined optimum geometries for rectilinear diffusers with rectangular, conical, or annular cross-sectional. *Fluid Mechanics of Internal Flow*, proceedings of a symposium held at General Electric Research Labs, 1967, 270–319.

17 Miller, D. S. Internal flow: a guide to losses in pipe and duct systems. The British Hydromechanics Research Association, 1971.